D0 Note 5099-CONF

Top Mass Measurement in the Lepton+Jets Channel using the Ideogram Method

The D0 Collaboration
URL http://www-d0.fnal.gov
(Dated: May 26, 2006)

A measurement of the top quark mass using the Ideogram technique is presented. This technique aims to optimize the use of statistical information by calculating an analytical likelihood for each event, while improving the reconstruction of the events using a kinematic fit. We select events with one charged lepton (electron or muon), missing transverse energy, and jets in the final state. The likelihood takes into account all possible jet assignments and the probability that an event was signal or background. To reduce the systematic uncertainty due to jet energy scale calibration, the invariant mass of the jets from the hadronically decaying W boson in the top quark candidate events is used to fit the jet energy scale in situ. Lifetime-based identification of b-jets is employed to enhance the separation between $t\bar{t}$ signal and background from other physics processes, and to improve the assignment of the observed jets to the partons in the $t\bar{t}$ hypothesis. Events with and without b-tags are included in the combined fit. This result is based on $370\,\mathrm{pb}^{-1}$ of data from $p\bar{p}$ collisions at a center-of-mass energy of 1.96 TeV, collected by the D0 experiment at the Fermilab Tevatron collider. With 116 events selected in the electron+jets channel and 114 in the muon+jets channel, the top quark mass is measured to be:

$$m_{\mathrm{t}} = 173.7 \pm 4.4\ (\mathrm{stat} + \mathrm{JES})^{+2.1}_{-2.0}\ (\mathrm{syst})\ \mathrm{GeV}$$

Preliminary result for the 2006 spring conferences

I. INTRODUCTION

We present a measurement of the mass of the top quark in the ℓ+jets channel, using the Ideogram method. The analysis presented here is an update of an earlier preliminary result [1]. It incorporates several major improvements in the analysis technique, and is applied to a larger data set. The current result uses 370 pb^{-1} of data collected by the D0 experiment from $p\bar{p}$ collisions at a center-of-mass energy of 1.96 TeV at the Fermilab Tevatron.

A constrained fit is used to solve the kinematics of the events and improve their reconstruction beyond the detector resolution. A likelihood is derived for every event including all possible assignments of jets to quarks in the $t\bar{t}$ hypothesis, and taking into account the possibility that the event was background. The top quark mass is extracted through a combined likelihood fit over all events. Free parameters in the fit are the top quark mass, the $t\bar{t}$ signal fraction in the sample, and an overall Jet Energy Scale (JES) factor. The JES calibration uncertainty has typically been one of the largest sources of systematic uncertainty in the top quark mass measurement. Including the JES factor as a free parameter in the fit greatly reduces this source of uncertainty.

Another major improvement in the current analysis is the use of b-tagging to enhance the separation between signal events and backgrounds from other physics processes. The b-tags are also used to better distinguish between correct and wrong jet assignments in the likelihood. Events with and without b tags are included in the overall likelihood fit.

II. COMMON DATA SET

This note describes the analysis of 370 pb^{-1} of data taken between April 2002 and August 2004. The event reconstruction and basic event selection are identical to what was used in the topological cross section analysis in the ℓ+jets channel [4], and the top quark mass measurement using the Matrix Element method [5, 6]. The basic selection requires an isolated lepton of high transverse momentum, $p_T > 20$ GeV, with a pseudo-rapidity $|\eta| < 1.1$ for electrons and $|\eta| < 2$ for muons. A significant missing transverse energy $\not\!\!E_T > 20$ GeV is required as well as four or more jets with $p_T > 20$ GeV and $|\eta| < 2.5$. In contrast to the Matrix Element analysis no veto is applied to remove events with more than four jets. A $\Delta\phi$ cut between $\not\!\!E_T$ and lepton momentum is imposed to exclude events where the transverse energy imbalance was caused by a poor measurement of the lepton energy.

III. JET ENERGY SCALE

The official D0 jet energy corrections are applied to all jets in the events. The jet response after these corrections was studied with a high-statistics sample of γ+jets events. The following variable is used to probe the p_T balance in these events:

$$\Delta S = \frac{p_T^{\rm jet} - p_T^{\gamma}}{p_T^{\gamma}} \tag{1}$$

Using the photon energy scale which is well known from $Z \to ee$ events, additional η-dependent corrections to the jet response were derived separately for data and Monte Carlo simulation. These η-dependent corrections give a uniform response as a function of η without changing the average normalization $\langle \Delta S \rangle$ for data or Monte Carlo simulation. The η-dependent corrections were applied to all jets in the $t\bar{t}$ sample and propagated to the $\not\!\!E_T$ before the final event selection.

The relative difference in jet energy scale between data and Monte Carlo simulation is the quantity of interest in the top quark mass measurement since the method to extract the top quark mass is calibrated with respect to the Monte Carlo simulation jet energy scale. To compare the difference in response between data and Monte Carlo (MC) simulation (in bins of p_T and η) the difference $\mathcal{D}$ defined as:

$$\mathcal{D} = \langle \Delta S \rangle_{\rm data} - \langle \Delta S \rangle_{\rm MC} \tag{2}$$

was parameterized as a function of photon p_T. The observed p_T-dependent difference $\mathcal{D}(p_T)$ between data and Monte Carlo simulation in bins of η is not used as a constraint in the top quark mass fit. However, it will be demonstrated that the result obtained with the jet+photon calibration is consistent with the Jet Energy Scale that is measured in situ, using the $t\bar{t}$ event sample.

The same approach that is used in the Matrix Element analysis is employed here: $\mathcal{D}$ is assumed to be a constant, independent of jet p_T and η, but no prior knowledge of the value of this constant is assumed in the top quark mass fit. Instead the top quark mass fit purely relies on the in-situ information from the invariant mass of the hadronically decaying W bosons in the $t\bar{t}$ events to set the Jet Energy Scale. A uniform Jet Energy Scale factor JES is introduced as

a free parameter in the overall fit, and this factor is fitted simultaneously with the top quark mass. The assumption that $\mathcal{D}$ is independent of the jet p_T is compatible with the jet+photon calibration. Nevertheless, the effects of a potential p_T dependence are taken into account as a systematic uncertainty. The analysis is calibrated such that in pseudo-experiments with Monte Carlo events (with η-corrections as described above) the average fitted JES value is equal to 1. A fitted value $JES < 1$ means that the jet energies in the sample considered are underestimated with respect to the reference Monte Carlo scale described above ($JES < 1$ is equivalent to $\mathcal{D} < 0$ when fitting the data sample).

IV. KINEMATIC FIT AND FINAL SELECTION

The jet correction procedure explained in section III corrects the measured jets for the portion of the showers which spread inside the jet cone, but not for radiation outside the cone. In the kinematic fit we aim to further correct the jet energies to those of the unfragmented partons in the MC. To this end, parton level corrections are applied, which are the same in data and MC simulation. The corrections depend on the flavor (b or light quark) of the parent quark and therefore depend on the jet-to-parton assignment used. To derive these parton level corrections we use MC events where the jets could be unambiguously matched matched to the partons of the $t\bar{t}$ decay and compare the jet energy to the parton energy according to the MC truth information. All parton-level corrections contain the JES parameter as a uniform multiplicative factor.

The kinematics of the events including the missing neutrino are reconstructed using the same kinematic constrained fit that was developed for the Run I 'template' analysis [7], but with resolutions updated to correspond to the Run II detector, as in [1, 8, 9]. In events with more than four jets, only the four jets with highest p_T are considered as possible candidates to be a light quark or b-quark in the $t\bar{t}$ hypothesis used in the constrained fit. All 12 possible assignments of jets to quarks are considered. When the event kinematics yield two solutions for the momentum of the neutrino in the direction of the beam, both solutions are used as a starting point for the fit, giving a maximum of 24 different fit solutions per event. Also extracted for each fit i from the kinematic fit are the estimated uncertainty on the fitted mass σ_i and the goodness of fit χ^2_i. The fit is repeated for different values of the JES parameter. The JES parameter is varied in steps of 3% in an interval of $\pm 15\%$ around 1. Only jet combinations are taken into account for which the fit converges at all values of JES. The fitted mass $m_i(JES)$, estimated uncertainty $\sigma_i(JES)$, and goodness of fit $\chi^2_i(JES)$ all depend on the JES parameter. In the following this dependence is not shown explicitly, to improve readability.

The final selection requirement is that at least one jet/neutrino solution yields $\chi^2 < 10$ for the kinematic fit with JES=1. This cut reduces the number of events from 120 to 116 in the electron+jets channel and from 126 to 114 in the muon+jets channel.

V. B-TAGGING AND SAMPLE COMPOSITION

This analysis employs lifetime tagging of b quark jets, using the same lifetime tagging algorithms that were used in the b-tagged cross section measurement in the ℓ+jets channel [10], the search for right-handed W bosons by D0 in Run II [9] and the Matrix Element analysis with b-tagging [6]. The identification of b jets is used to improve the separation between signal and background events (see below), and to better distinguish between 'correct' and 'wrong' jet assignment hypotheses. Events with 0, 1, or ≥ 2 b-tagged jets are all used in a combined fit.

In order to obtain an optimal separation between $t\bar{t}$ signal and (mainly W+jets) backgrounds without biasing the top quark mass measurement, a likelihood discriminant based on the 'low-bias' topological discriminant $D_{\rm LB}$ was used, developed in Run I [7]. The low-bias discriminant is based on 4 topological variables whose definition is given in [8]. The discriminant was designed to obtain good separation between $t\bar{t}$ and background events with minimal correlation with the fitted top quark mass. For the analysis presented here, the low-bias discriminant $D_{\rm LB}$ ($\equiv x_1$) was combined with a new variable called 'p_T-fraction' and the number of b-tags. The 'p_T-fraction', defined as: $x_2 = (\sum_{\rm tracksinjets} p_T)/(\sum_{\rm alltracks} p_T)$, is the p_T-weighted fraction of all tracks in the event that point at a jet (with jet p_T >20 GeV within $-2.5 < \eta < 2.5$). Only those tracks wer considered that have a distance of closest approach of less than 1 cm in the z-direction with respect to at least one of the primary vertices in the event.To point at a jet, the track was required to point within a cone of 0.5 in detector-η and ϕ from the center of the jet. This variable distinguishes clean events with nicely collimated jets from events with broader jets and significant underlying hadronic activity. Finally, x_3 is the number of b-tags. To good approximation these 3 variables are uncorrelated, and

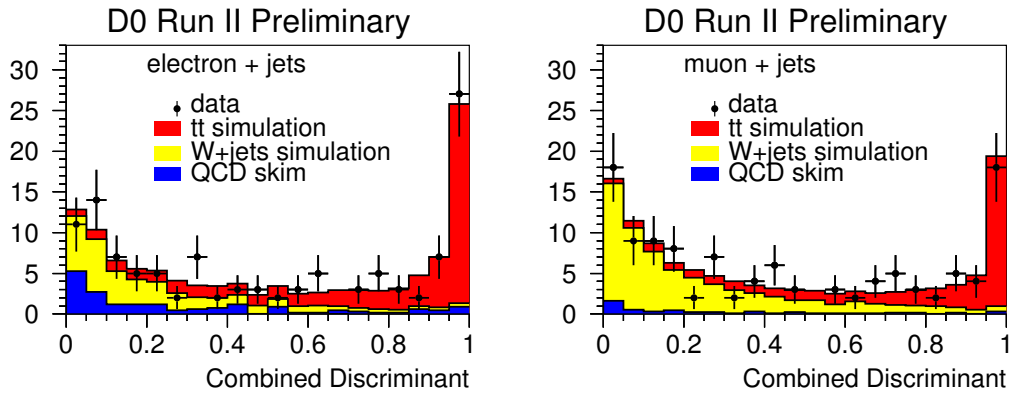

FIG. 1: *Combined likelihood discriminant in data and MC in the electron+jets channel (left) and muon+jets channel (right).*

a combined likelihood discriminant is derived as

$$D_{\text{combined}} = \frac{\Pi_i s_i(x_i)/b_i(x_i)}{\Pi_i s_i(x_i)/b_i(x_i) + 1}, \tag{3}$$

thus combining topological with a tracking-based jet shape and b-tag information. This combined likelihood discriminant offers a much better discrimination between $t\bar{t}$ and backgrounds than does the low-bias topological variable D_{LB} by itself, while maintining its low level of correlation with the fitted top quark mass (and therefore with the jet energy scale).

Figure 1 shows the distribution of the discriminant obtained in the electron+jets and muon+jets channels. The distribution observed in data is compared to the MC simulation. The simulated sample consists of $t\bar{t}$ and W+jets events generated with ALPGEN and a QCD (multi-jets) enriched sample obtained from data by inverting the lepton isolation cut in the event selection. A likelihood fit was performed to determine the estimated fraction of $t\bar{t}$ events. The fit results are shown in Table I. In the fit the ratio between the number of QCD and W+jets events was kept fixed to a value based on the estimate used in [4–6].

	electron+jets	muon+jets
no. of events observed in data	116	114
estimated sample composition:		
$t\bar{t}$	61.5 ± 8	45.6 ± 8
W+jets	35.6 ± 5	63.0 ± 8
QCD	18.9 ± 3	5.4 ± 1

TABLE I: *Estimated sample composition of the 370 pb^{-1} data sample.*

VI. THE IDEOGRAM METHOD

To maximize the statistical information on the top quark mass extracted from the event sample, a likelihood to observe the event is calculated for each event as a function of the assumed top quark mass m_{top}, the jet energy scale factor JES and fraction of $t\bar{t}$ events in the event sample, f_{top}. The likelihood is composed of two terms, describing the hypotheses that the event was $t\bar{t}$ signal, or an event originating from a background process:

$$\mathcal{L}_{\text{evt}}\left(x; m_{\text{top}}, JES, f_{\text{top}}\right) = f_{\text{top}} \cdot P_{\text{sgn}}\left(x;\, m_{\text{top}}, JES\right) + \left(1 - f_{\text{top}}\right) \cdot P_{\text{bkg}}\left(x;\, JES\right) \ . \tag{4}$$

Here, x denotes the full set of observables that characterize the event, $f_{\rm top}$ is the signal fraction of the event sample, and $P_{\rm sgn}$ and $P_{\rm bkg}$ are the probabilities for $t\bar{t}$ and W+jets production, respectively. Contributions from QCD multijet events are not treated explicitly and are considered as a systematic uncertainty. The event observables x can be divided in two groups. One set was chosen to provide good separation between signal and background events while minimizing the correlation with the mass information in the event. These variables (topological variables and b-tagging) were used to construct a low-bias combined discriminant D, as described in section V. The other event information used is the mass information $x_{\rm fit}$ from the constrained kinematic fit, which provides the sensitivity to the top quark mass and jet energy scale. To good approximation D is uncorrelated with $x_{\rm fit}$ and with the jet energy scale. Thus the probabilities $P_{\rm sgn}$ and $P_{\rm bkg}$ can be written as the product of a probability to observe a value D and a probability to observe $x_{\rm fit}$, as

$$P_{\rm sgn}\left(x;\, m_{\rm top}, JES\right) \equiv P_{\rm sgn}\left(D\right) P_{\rm sgn}\left(x_{\rm fit};\, m_{\rm top}, JES\right) \tag{5}$$

and

$$P_{\rm bkg}\left(x;\, JES\right) \equiv P_{\rm bkg}\left(D\right) P_{\rm bkg}\left(x_{\rm fit};\, JES\right) \tag{6}$$

where D is calculated for a JES parameter equal to 1. The normalized probability distributions of the discriminant D for signal $P_{\rm sgn}\left(D\right)$ and background $P_{\rm bkg}\left(D\right)$ are assumed to be independent of JES and are obtained from Monte Carlo simulation as discussed in section V. They correspond to parameterized versions of the Monte Carlo templates shown in Figure 1. The reconstruction of the signal and background probabilities for the mass information $x_{\rm fit}$ is explained below. The mass information in the event $x_{\rm fit}$ consists of all fitted masses $m_i(JES)$, estimated uncertainty $\sigma_i(JES)$, and goodness-of-fit $\chi^2_i(JES)$ obtained from the kinematic fit.

A. Calculation of signal and background probability

The probabilities are calculated as a sum over all 24 possible jet/neutrino solutions. The relative probability for each of the solutions i to be correct is estimated as w_i. Without b-tagging, w_i purely depends on the χ^2_i for the corresponding fit and is defined as $w_i = \exp(-\frac{1}{2}\chi^2_i)$. To further improve the separation between correct and incorrect jet assignments, b-tagging is used. If one or more jets in the event are b-tagged an additional relative weight $w_{{\rm btag},i}$ is assigned, representing the probability that the observed b-tags are compatible with the jet assignment assumed for that particular jet permutation:

$$w_{{\rm btag},i} = \prod_{j=1,n_{\rm jet}} p^j_i \tag{7}$$

where p^j_i can either be ε_l, (1-ε_l), ε_b or (1-ε_b), depending on the assumed flavor of the jet (light or b) and whether or not that particular jet was tagged. Tagging rates for light and b-quark jets ε_l and ε_b, determined from data were used as parameterized functions of jet p_T and η, where the jet p_T is based on the reconstructed jet energy for $JES = 1.00$, consistent with [10]. Thus, the weight assigned to each jet combination becomes

$$w_i = \exp(-\frac{1}{2}\chi^2_i) \prod_{j=1,n_{\rm jet}} p^j_i \tag{8}$$

The mass-dependent signal probability in Equation 5 is calculated as

$$P_{\rm sgn}\left(x_{\rm fit};\, m_{\rm top}, JES\right) \equiv \sum_{i=1}^{24} w_i \left[f^{\rm ntag}_{\rm correct} \cdot \int_{100}^{300} \mathbf{G}(m_i, m', \sigma_i) \cdot \mathbf{BW}(m', m_{\rm t}) dm' + (1 - f^{\rm ntag}_{\rm correct}) \cdot {\rm S}^{\rm ntag}_{\rm wrong}(m_i, m_{\rm t}) \right] \tag{9}$$

and the background term (Equation 6):

$$P_{\rm bkg}\left(x_{\rm fit};\, JES\right) \equiv \sum_{i=1}^{24} w_i \cdot BG(m_i) \tag{10}$$

The signal term consists of two parts: one part describes the compatibility of the solution with a certain value of the top quark mass, if that solution indeed is the correct solution, taking into account the estimated mass resolution σ_i for each jet permutation. The second part of the signal term describes the expected shape of the mass spectrum

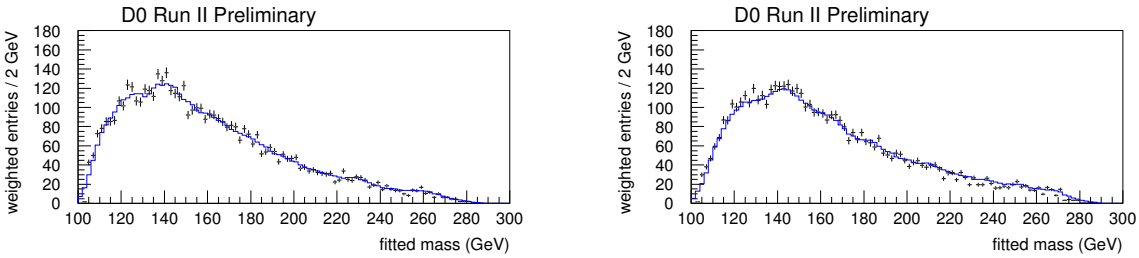

FIG. 2: *These histograms show the background shape from a weighted sum (see text) of all 24 masses from each event from the W+jets background sample (points with error bars), for the electron+jets channel (left) and muon+jets (right). The open histogram shows the shape that is used in the likelihood. To reduce statistical fluctuations this shape is calculated as the average value in a sliding window of ±5 GeV around each fitted mass.*

for the 'wrong' jet assignments, which also depends on the top quark mass. The 'correct' solution part is given by a convolution of a Gaussian resolution function $\mathbf{G}(m_i, m', \sigma_i)$ describing the experimental resolution with a relativistic Breit-Wigner $\mathbf{BW}(m', m_{\rm t})$, representing the expected distribution of the average of the two invariant masses of the top and anti-top quarks in the event, for a top quark mass $m_{\rm t}$. The 'wrong' permutation signal shape $\mathrm{S}^{\rm ntag}_{\rm wrong}(m_i, m_{\rm t})$ is obtained from MC simulation using a procedure described in section VI B. These two terms are assigned a relative weight depending on the probability $f^{\rm ntag}_{\rm correct}$, which represents the relative probability that the weight is assigned to the correct jet permutation, which is $\approx 39\%$ if b-tagging is not used, for well-reconstructed events with exactly 4 jets. For untagged 4-jet events a value $f^0_{\rm correct}$=0.45 was used. For 4-jet events with one or more than one b-tag, the values $f^1_{\rm correct}$=0.55 and $f^2_{\rm correct}$=0.65 turned out to give good performance. For 5-jet events smaller fractions are used: 0.15, 0.30 and 0.40 for events with 0, 1, or ≥ 2 b-tagged jets respectively.

For the background term a weighted sum $\mathrm{BG}(m_i)$ is used, where $\mathrm{BG}(m)$ is the shape of the mass spectrum obtained from W+jets in MC simulation with all entries weighted according to the permutation weight w_i assigned to each solution, and a value of JES equal to unity. The $\mathrm{BG}(m)$ shapes used in the analysis can be seen in Figure 2.

The Breit-Wigner and 'wrong' permutation signal shape are normalized to unity on the integration interval: 100 to 300 GeV. This interval was chosen large enough so as not to bias the mass in the region of interest. The normalization of the background shape $\mathrm{BG}(m_i)$ is calibrated to minimize the offset in the fitted purity, in the region of interest around the expected signal fraction of 0.45. A constant normalization factor of 1.15 was found to give offsets in fitted signal fraction smaller than 1% both in the electron+jets and the muon+jets channel. The jet energy scale parameter is varied before performing the constrained fit by scaling all jet energies with a constant factor, and the event likelihoods are recalculated for each different value of the JES factor. Since the constrained fit uses a W boson mass constraint (m_W = 80.4 GeV), the χ^2 in the fit will be best when the invariant mass of the jets from the hadronically decaying W boson is closest (on average) to the known W boson mass. Additional sensitivity to the jet energy scale comes from the shape of the fitted mass distribution in background events. For the proper jet energy scale the spectrum will agree best with the background shape included in the background term in the likelihood. Since each event is independent the combined likelihood for the whole sample is calculated as the product of the single event likelihood curves:

$$\mathcal{L}_{\rm samp}(m_{\rm t}, JES, f_{\rm top}) = \prod_j \mathcal{L}_{{\rm evt}j}(m_{\rm t}, JES, f_{\rm top}) \tag{11}$$

This likelihood is maximized with respect to the top quark mass $m_{\rm t}$, the jet energy scale JES, and the estimated fraction of signal in the sample $f_{\rm top}$.

B. Determination of the Wrong-Permutation Signal Shape

The convolution of Gaussian detector resolution and a Breit-Wigner used in the signal term of the likelihood implicitly assumes that the correct jet assignment was chosen. To describe the contribution from 'wrong' jet assignments a separate term is added to the signal part of the likelihood. To obtain the fitted mass spectrum of the wrong permutations signal, samples of parton-matched $t\bar{t}$ events were used, in which all quarks were matched to jets. The fitted mass spectrum was plotted including all jet permutations *except* the correct solutions (excluding both neutrino solutions

corresponding to the correct jet permutation), with each entry weighted according to the permutation weight assigned in the Ideogram likelihood. Samples of different generated top quark masses were used. For each mass the weighted sum of wrong solutions was fitted with a double Gaussian. The fitted parameters for correct solutions and for the wrong permutation signal show a nice linear development as a function of the top quark mass. The fitted parameters are given in Table II.

These linear fits were then used to construct a 2-dimensional background shape as a function of the fit mass, and generated top quark mass, $S^{\rm ntag}_{\rm wrong}(m_i, m_{\rm t})$, where for each value of the top mass the shape as a function of fitted mass is described as the sum of two Gaussians.

Since the permutation weights change when b-tagging is included, this exercise was repeated for events with 0 tags, 1 tag, and 2 or more tags. In Figure 3 the parameterized shapes of the correct solutions and wrong solutions are shown, and the sum of the two is compared the weighted histogram of all fitted masses. In Figure 4 the corresponding distributions are shown for events with 0, 1, or 2 tags. It is clearly visible how the fraction of weight given to the correct solution improves when including b-tag information in the permutation weights.

	0 tags				1 tag				2 tags			
	Gauss 1		Gauss 2		Gauss 1		Gauss 2		Gauss 1		Gauss 2	
	$p0$	$p1$	$p0$	$p1$	$p0$	$p1$	$p0$	$p1$	$p0$	$p1$	$p0$	$p1$
a	284.9	-1.722	51.72	-0.4199	267.5	-1.0700	68.08	-0.7129	235.5	-0.1662	75.86	-0.0415
mean	161.7	0.7383	223.1	1.242	162.6	0.7859	220.1	1.400	166.2	0.6416	229.4	0.7454
σ	23.55	0.2392	22.94	-0.2528	23.27	0.2737	23.97	-0.4551	25.80	0.1165	21.78	-0.2828

TABLE II: *Parameters used to describe the background shapes (arbitrary normalization). For each case, the shape is described by 2 Gaussians* $G(m_{\rm fit}) = a \cdot \exp(-(\text{mean} - m_{\rm fit})^2/2\sigma^2)$, *where the 3 parameters* a, *mean, and* σ *evolve linearly as a function of the generated top quark mass* m_t *as* $p0 + p1 \cdot (m_t - 175\ GeV)$.

C. Determination of JES offset correction

The likelihood fit relies on the invariant mass of the hadronically decaying W boson in the $t\bar{t}$ events to set the jet energy scale. It is designed to give an unbiased fit of the JES parameter in well-reconstructed $t\bar{t}$ events when the correct jet assignment is used. However, in a significant fraction of the events the supposed jets from the W boson may not really come from a W boson with an invariant mass equal to the constraint (=80.4 GeV) used in the fit. Such cases include events other than $t\bar{t}$ or $t\bar{t}$ events that were misreconstructed. In the presence of such events there is no a priori reason to expect the JES parameter to be fitted without offset. The slope of the JES calibration curve (fitted JES parameter as a function of the 'true' JES) may also differ from unity. Such effects need to be investigated carefully and corrected for.

Using the MC calibration procedure described in the next section (see section VI D) it was found that the presence of wrong jet assignments and background events indeed causes an offset of several percent in the fitted JES parameter. A breakdown of the different contributions to JES offset and slope is shown in Table III.

	JES slope	JES offset	expected mass error after full calibration
parton-matched $t\bar{t}$ only	0.96	+0.026	
all $t\bar{t}$	0.88	+0.050	
all $t\bar{t}$ and W+jets	0.80	+0.076	4.30 GeV
all $t\bar{t}$ and W+jets, with 50% offset correction	0.72	+0.036	4.10 GeV
all $t\bar{t}$ and W+jets, with 100% offset correction	0.63	+0.000	4.01 GeV

TABLE III: *The JES offset increases and JES calibration slope becomes smaller when adding mis-reconstructed signal events and background events. Correcting for the offset at likelihood level (see text) fixes the JES offset but further reduces the JES calibration slope.*

Fortunately it turns out that the JES offset and slope are independent of the generated top quark mass (see also section VI D). Therefore it is straightforward to apply a correction which is independent of the top quark mass. An ad-hoc normalization factor $f_{\rm JES}(JES, f_{\rm top}) = \exp(a \cdot JES)$ corrects the offset without changing the statistical uncertainty estimated from the likelihood (in case the final sample likelihood is Gaussian):

$$\mathcal{L}^{\rm corr}_{\rm evt}(m_{\rm t}, JES, f_{\rm top}) = f_{\rm JES}(JES, f_{\rm top}) \cdot \mathcal{L}_{\rm evt}(m_{\rm t}, JES, f_{\rm top}). \quad (12)$$

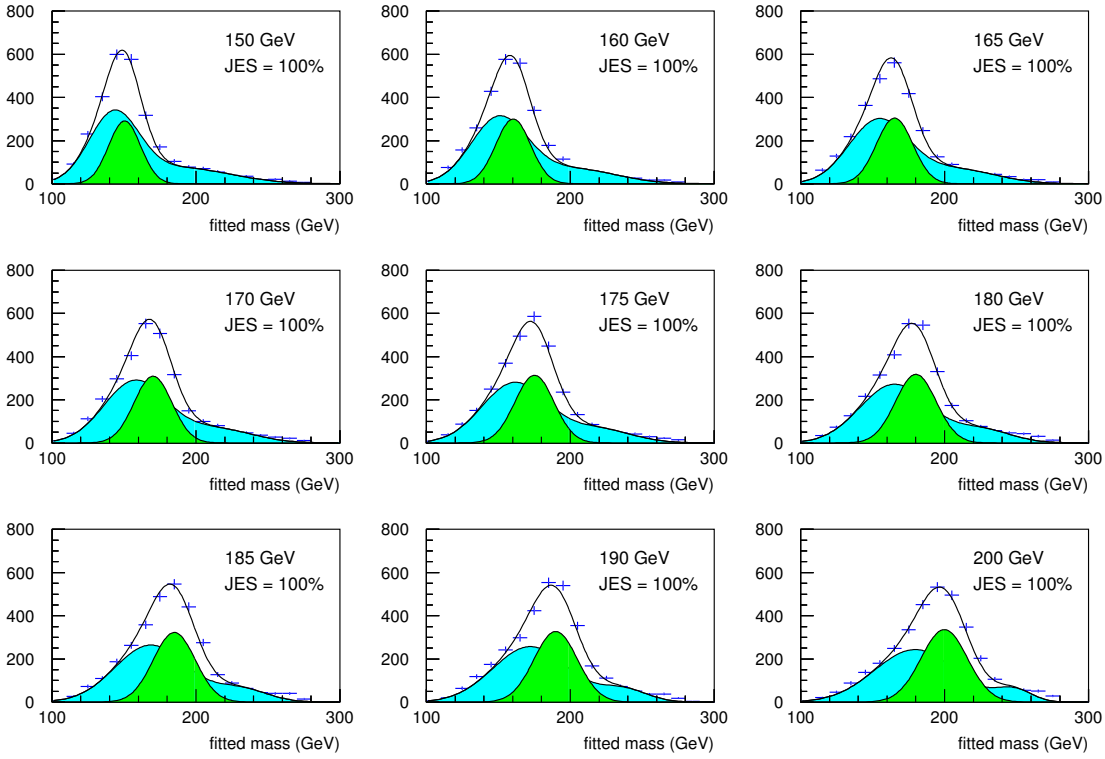

FIG. 3: *Using the fitted parameters shown in Table II, the wrong permutation shape (blue or light shade) and the shape of the correct solutions (green or darker shade) is predicted at each top quark mass, and the sum of the two (black line) is compared to the histogram containing a weighted sum of all solutions (correct and wrong), for the default jet energy scale.*

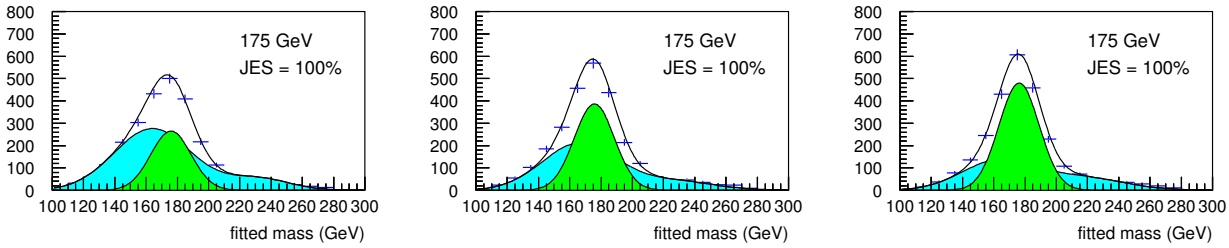

FIG. 4: *Same as Figure 3, for a generated top quark mass of 175 GeV for events with 0 (left), 1 (middle), or more than 1 (right) b-tags.*

Since background events on average cause a larger bias than signal events, the value of a is defined as being dependent on the measured signal fraction: $a = 2.63 + 0.56(1 - f_{\rm top})$, where $f_{\rm top}$ is the measured signal fraction. The value of the correction constants was tuned using MC simulation, to give an unbiased measurement of the JES at the reference scale JES = 1.0. As shown in Table III the application of this offset correction does remove the JES offset, but at the cost of a further reduced JES slope. The Table also shows that after full calibration (described in the next section), the expected statistical uncertainty on the top quark mass improves when applying the corrections.

The correction described above ensures that the fit is well behaved and that for values of the JES close to 1.0 the fit results will stay well within the range for which the (JES, m_t) likelihood is calculated. It does not provide a full

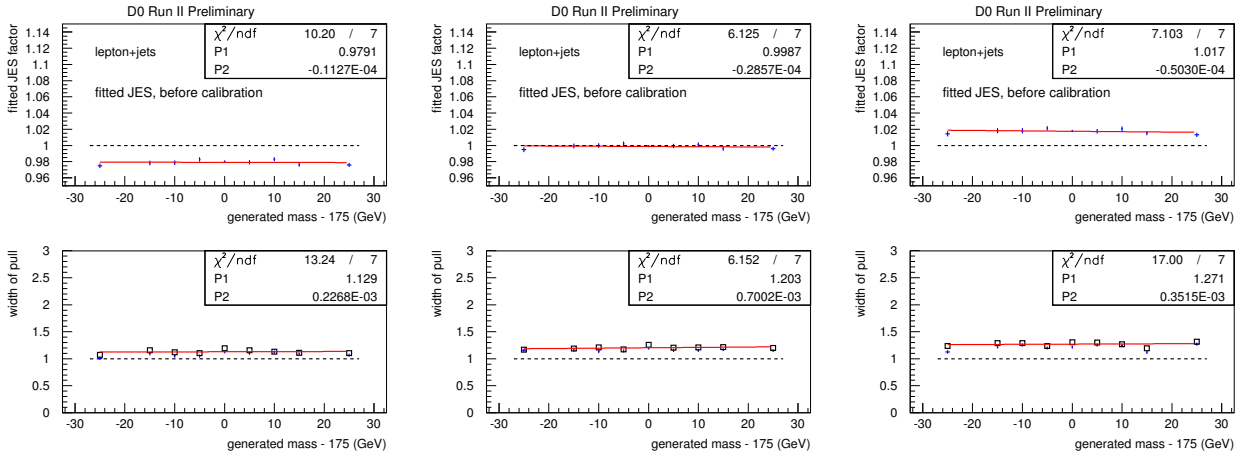

FIG. 5: *The mean fitted JES before calibration is shown as a function of the generated top quark mass for a 'true' JES of 0.97 (left), 1.00 (middle), and 1.03 (right), for the lepton+jets channel. The fitted JES is very stable as a function of generated top quark mass. The calibration slope for the fitted vs. true JES is 0.63 at 175 GeV and varies less than 0.01 over the whole range.*

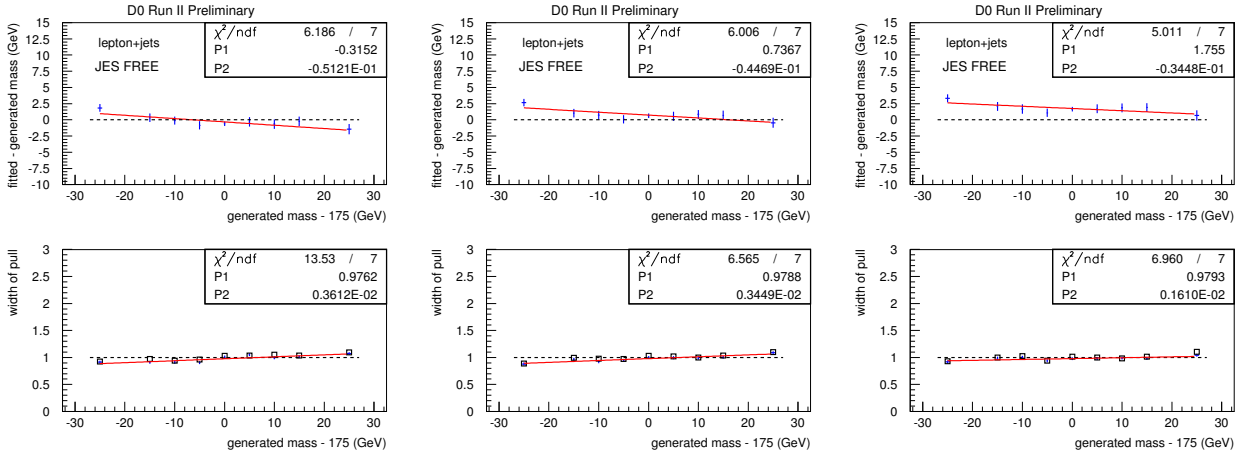

FIG. 6: *The mean fitted mass before calibration is shown as a function of the generated top quark mass for a 'true' JES of 0.97 (left), 1.00 (middle), and 1.03 (right), for the lepton+jets channel. At a generated mass of 175 GeV the mass bias changes only by 1 GeV when the true JES is varied by ±3%.*

calibration of the analysis, however. This is described in the following section.

D. Calibration using Monte Carlo simulation

The analysis is calibrated using Monte Carlo simulation. Both the bias on the measured mass and the correctness of the estimated statistical uncertainty can be tested using ensemble testing, where each ensemble corresponds to a simulated experiment corresponding to the size of the data sample. Thousands of ensembles were constructed, combining $t\bar{t}$ and W+jets from MC simulation. The fractions of $t\bar{t}$ and W+jets were allowed to fluctuate according to binomial statistics around the estimated fractions in the actual data sample. The fractions used are the ones listed in Table I. The total sample size was fixed to the observed number of events in data (116 in electron+jets and 114 in muon+jets). To make optimal use of the available MC statistics, standard resampling techniques were used, allowing for the multiple use of MC events when constructing the ensembles [19, 20].

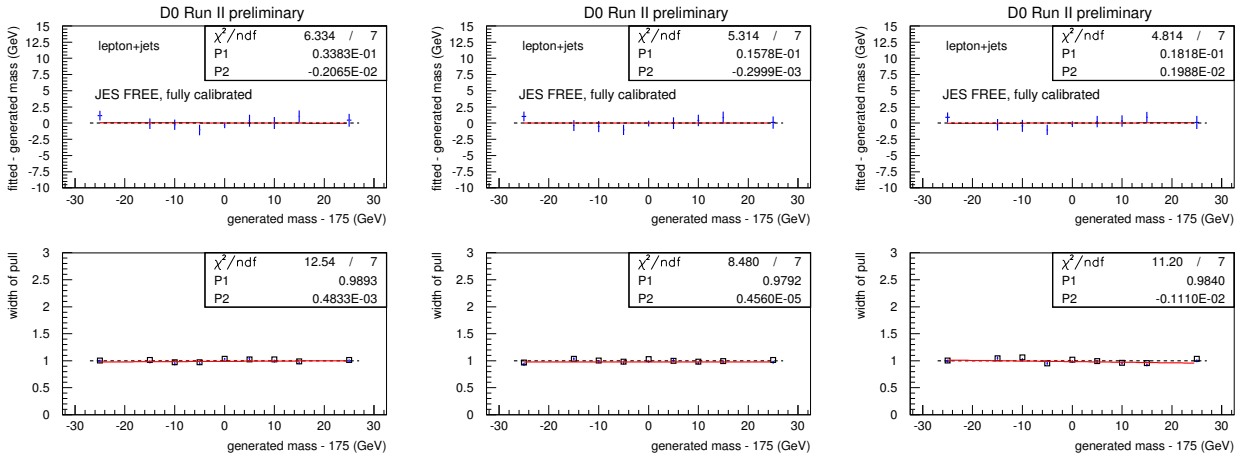

FIG. 7: *The mean fitted mass after full calibration is shown as a consistency check, as a function of the generated top quark mass for a 'true' JES of 0.97 (left), 1.00 (middle), and 1.03 (right), for the lepton+jets channel.*

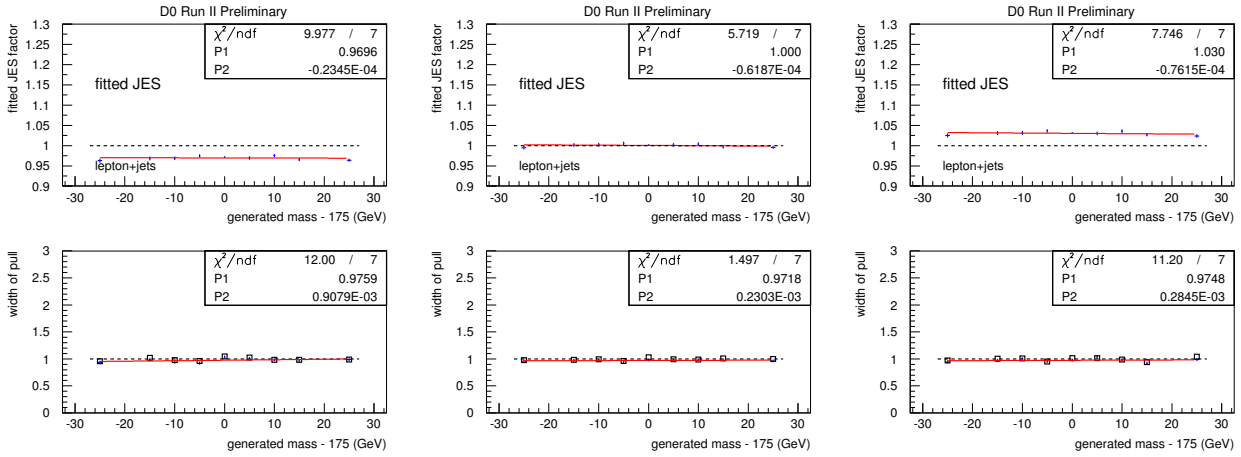

FIG. 8: *The mean fitted JES after full calibration is shown as a consistency check, as a function of the generated top quark mass for a 'true' JES of 0.97 (left), 1.00 (middle), and 1.03 (right), for the lepton+jets channel.*

Figure 5 shows how the fitted JES behaves as a function of the top quark mass for different values of the true jet energy scale. The fitted JES factor is independent of the top quark mass over the full range considered. The plots also show that the fitted JES changes linearly as a function of the true JES with a slope of 0.63. Figure 6 shows the corresponding change in fitted top quark mass as a function of the true JES. Using these plots a full two-dimensional calibration can be performed, describing the fitted JES and top quark mass as a function of the 'true' JES and top quark mass generated in the MC simulation. As a consistency check Figures 7 and 8 demonstrate that after calibration the fitted top quark mass and JES become bias free, with a width of the pull that is everywhere equal to unity, indicating that the statistical uncertainties are correctly estimated.

E. Alternative calibration strategies

Including the uniform JES factor as a free parameter in the fit reduces the systematic uncertainty due to the jet energy scale, at the cost of a larger statistical uncertainty. As a comparison in Figure 9 the mass calibration curves are shown for different values of the true JES, when the JES parameter in the fit is fixed to 1.0 (the dependence as a

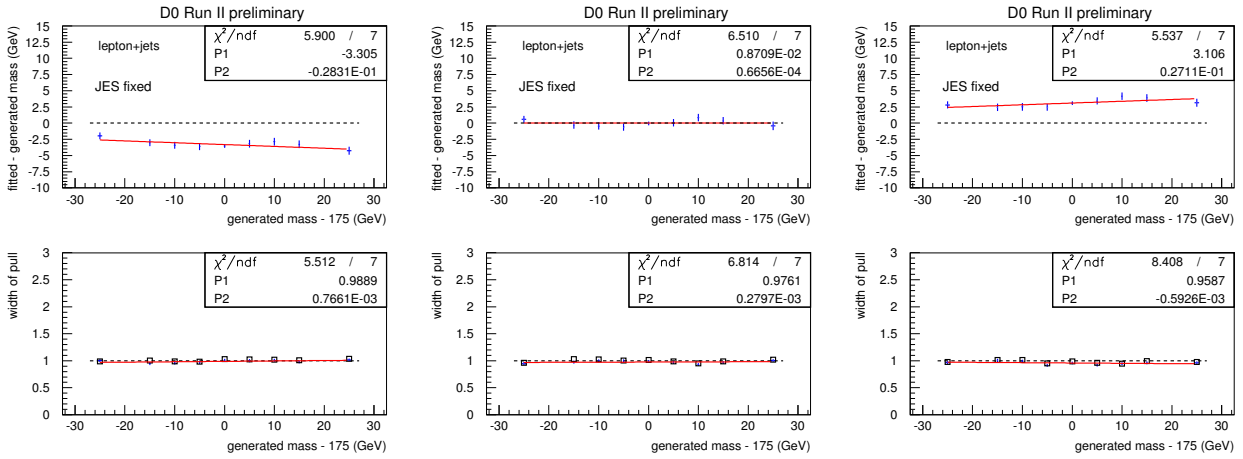

FIG. 9: *The mean fitted mass is shown as a function of the generated top quark mass for a 'true' JES of 0.97 (left), 1.00 (middle), and 1.03 (right), for the lepton+jets channel, when fixing the JES parameter in the fit to 1.0.*

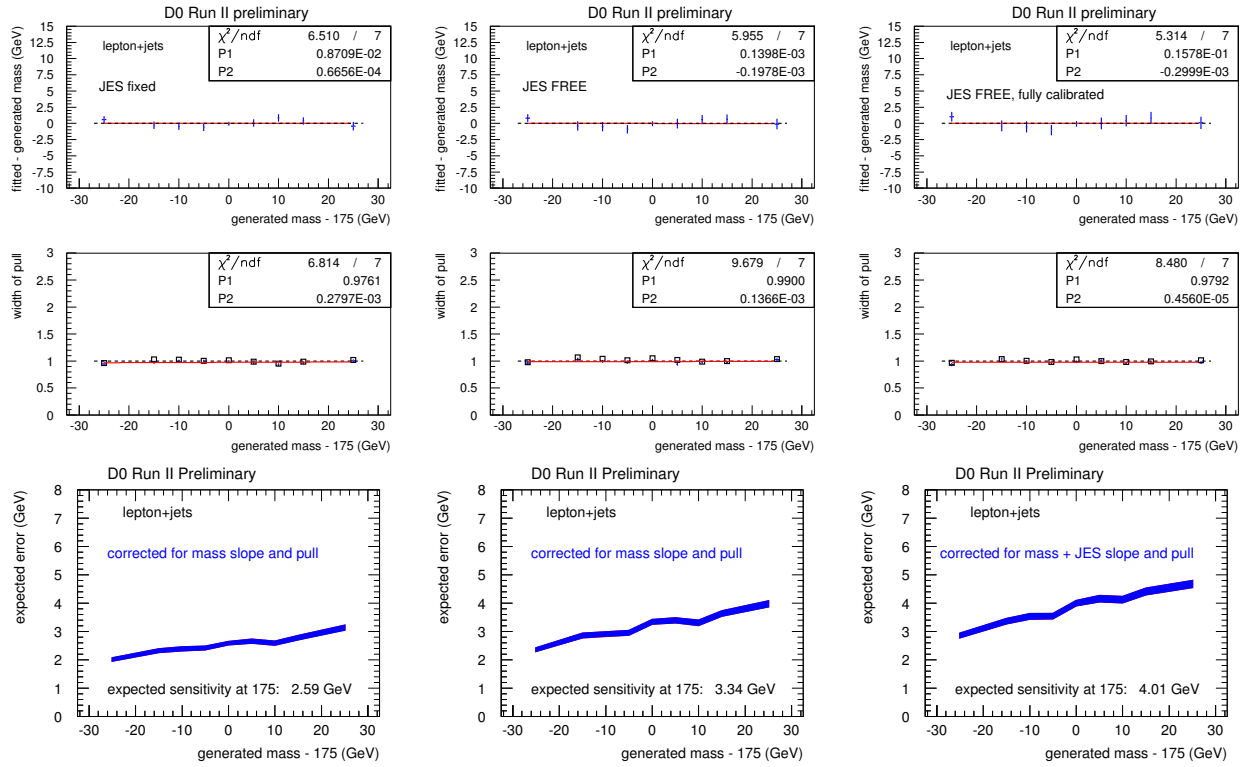

FIG. 10: *The mean fitted mass after calibration (top), width of the mass pull (middle) and expected statistical uncertainty (bottom) are shown as a function of the generated top quark mass for three scenario's: with the JES parameter fixed to 1.0 (left), allowing the JES parameter to float freely in the fit, but only calibrating the mass fit for a true JES=1.0 (middle), allowing the JES parameter to float freely in the fit and applying the full calibration as a function of true top quark mass and true JES (right).*

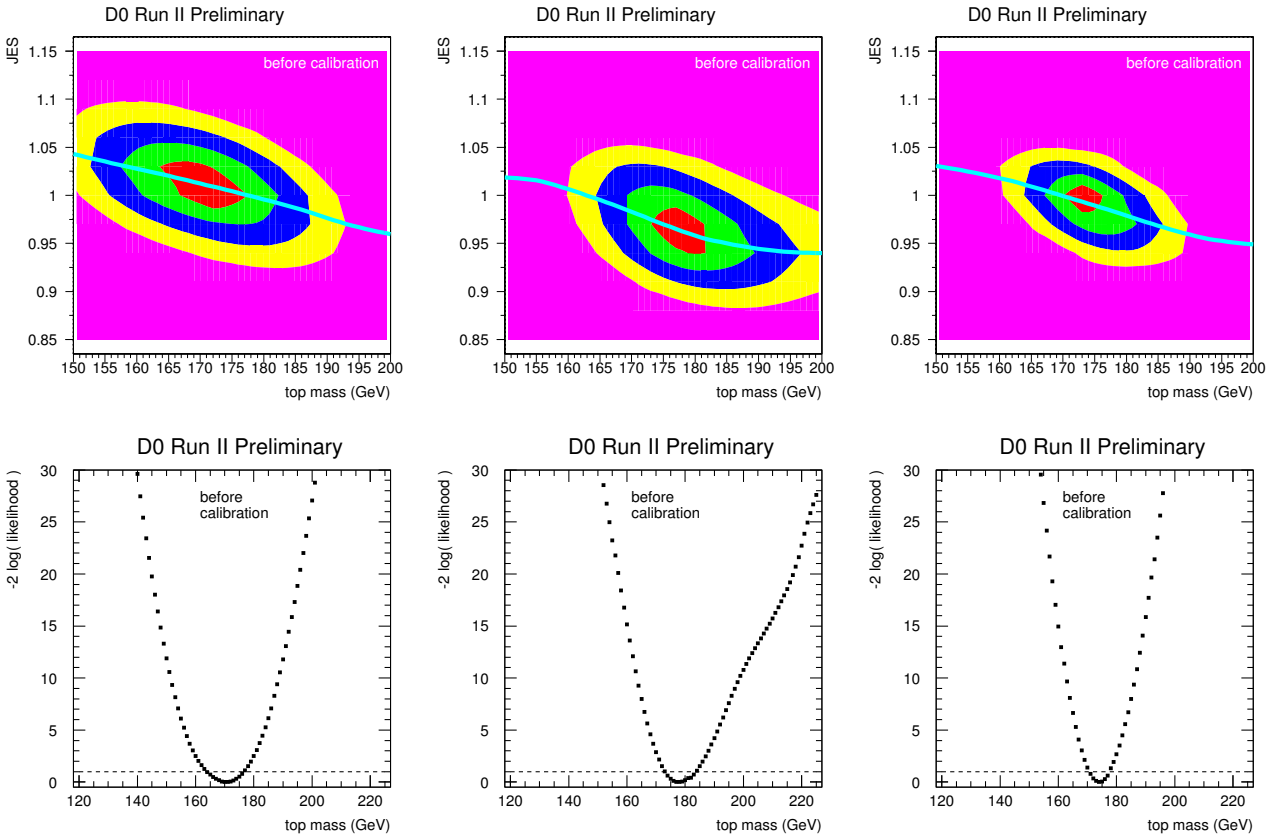

FIG. 11: *Overall likelihood curves for the events observed in data, in the electron+jets channel (left), muon+jets (middle), and both channels combined (right). The top plots show the full 2-dimensional likelihood as a function of the Jet Energy Scale factor (JES) and top quark mass. Each contour corresponds to a change of one unit in* $\sqrt{2ln(max\ likelihood)\text{-}2ln(likelihood)}$ *The bottom plots show the likelihood as a function of the top quark mass, fitting for the JES factor with maximum likelihood at each value of the mass. The fitted value of the JES factor as a function of the top quark mass is plotted as a blue line superimposed on the 2D likelihoods (top). These likelihood curves are shown before calibration.*

function of top quark mass and mass pull have been calibrated for a true JES=1.0). The change in mass bias (at 175 GeV) is about 3.2 GeV per 3% change in true JES. This is about a factor 3 larger than the mass dependence of 1.0 GeV per 3% that was seen in Figure 6, *before* JES calibration. This means that without correcting for the JES slope (=0.63) in the calibration, the analysis already 'absorbs' about $2/3 \approx 0.63$ of the JES and its effect on the mass in the fit. Since the jet energy scale is known from jet+photon studies with a few percent precision, a factor 3 reduction is sufficient to reduce the otherwise dominant JES systematic to the level of other systematic uncertainties. Fully calibrating the the analysis as a function of fitted mass and JES (the default approach) allows an unbiased top quark mass measurement for any value of the 'true' JES, at the cost of an even larger statistical uncertainty. The expected statistical uncertainties for the above three scenarios are compared in Figure 10.

In order to be consistent with the approach used by the Matrix Element analysis [18] and to minimize the dependence on the external JES constraint from jet+photon calibration, the third scenario is presented here as the main analysis result, applying the full calibration as a function of fitted top quark mass and JES. Results using the other two calibration methods will be quoted as a cross-check in section IX.

VII. RESULTS WITH DATA

The overall likelihood curves before calibration obtained in data are shown in Figure 11. The 2D likelihoods show the actual likelihood values in bins of 1 GeV in mass and 3% in JES. The jagged appearance of the ellipses is caused by the large bin size in JES direction. To extract the mass and statistical error a Gaussian fit is applied to the 3 bins

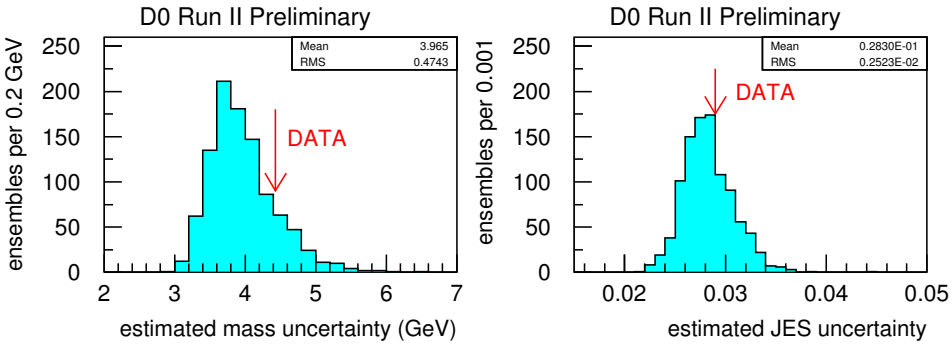

FIG. 12: *Distribution of the estimated statistical uncertainty on the top quark mass measurement (left) and JES measurement (right) for the fully calibrated analysis, in the lepton+jets channel. The values observed in data are indicated by the arrows.*

closest to the minimum in the 1-dimensional -ln(likelihood) curves. After full calibration the result fitted in data is:

$$m_t = 173.74 \pm 4.43 \text{ (stat + JES) GeV with JES} = 0.989 \pm 0.029$$

All uncertainties shown are statistical. The uncertainties observed in data agree well with the expectation from MC simulation, as shown in Figure 12. The fitted $t\bar{t}$ signal fraction is $45.3 \pm 3.2\%$ after calibration. If the JES parameter is kept fixed to 1.0 in the fit, the estimated statistical uncertainty is 2.93 GeV. One could therefore say that the 4.43 GeV (stat+JES) uncertainty of the 2D fit corresponds to an intrinsic mass uncertainty 2.93 GeV (stat) and an additional uncertainty of 3.32 GeV (JES) due to fitting the JES parameter. Only statistical uncertainties are shown here. The fitted JES of 0.989±0.029 is in good agreement with the reference scale 1.0 (or $\mathcal{D}$=0), corresponding to the hypothesis that after all official D0 jet corrections the JES in data and MC are the same.

One can also compare the in-situ fitted JES factor with the jet+photon calibration. When applying the measured jet-p_T dependent difference between data and MC simulation $\mathcal{D}(p_T)$ as a final correction to all jets in MC and redoing the ensemble tests in MC simulation, the mean fitted JES is 0.962+0.021-0.023, where the uncertainties correspond to the (stat+syst) one sigma bounds quoted in the jet+photon studies. This is in excellent agreement with the value of 0.989±0.029 measured in situ.

Finally, as an illustration Figure 13 shows the distributions of the values of the top quark mass and the JES parameter for which the event likelihood has its maximum value *per event*. Only events are included for which the combined discriminant D has a value larger than 0.3. The distribution in data is compared to the expectation from MC simulation for a true JES=1.0 and a generated top quark mass of 175 GeV, showing good agreement. Note that these plots only show one number per event and do *not* convey the full information that is taken into account in the actual likelihood fit.

VIII. SYSTEMATIC UNCERTAINTIES

The final calibration of the analysis relies on the Monte Carlo simulation for a detailed description of the physics processes involved and the detector performance. Any discrepancy between the Monte Carlo simulation and reality may lead to a miscalibration and thus to a systematic error on the measured top quark mass. Therefore, any possible discrepancy needs to be considered carefully. This was done by applying each effect one by one to the Monte Carlo simulation and redoing the ensemble tests, without changing the analysis itself, to determine the size of the shift in the calibration curve. The total systematic uncertainty on the top quark mass measurement was obtained by adding all contributions in quadrature. The following sources of systematics have been considered (also see Table IV):

- **JES p_T dependence:** The relative difference between the jet energy scales in data and Monte Carlo is fitted with a global scale factor, and the corresponding systematic uncertainty is included in the quoted (stat. + JES) error. Any discrepancy between data and simulation other than a global scale difference may lead to an additional uncertainty on the top quark mass. The uncertainty due to a possible jet-p_T dependent shape was estimated by scaling the energies of all jets in the MC with a factor $(1 + 0.02(p_T - 100\text{GeV}))$, where p_T is the

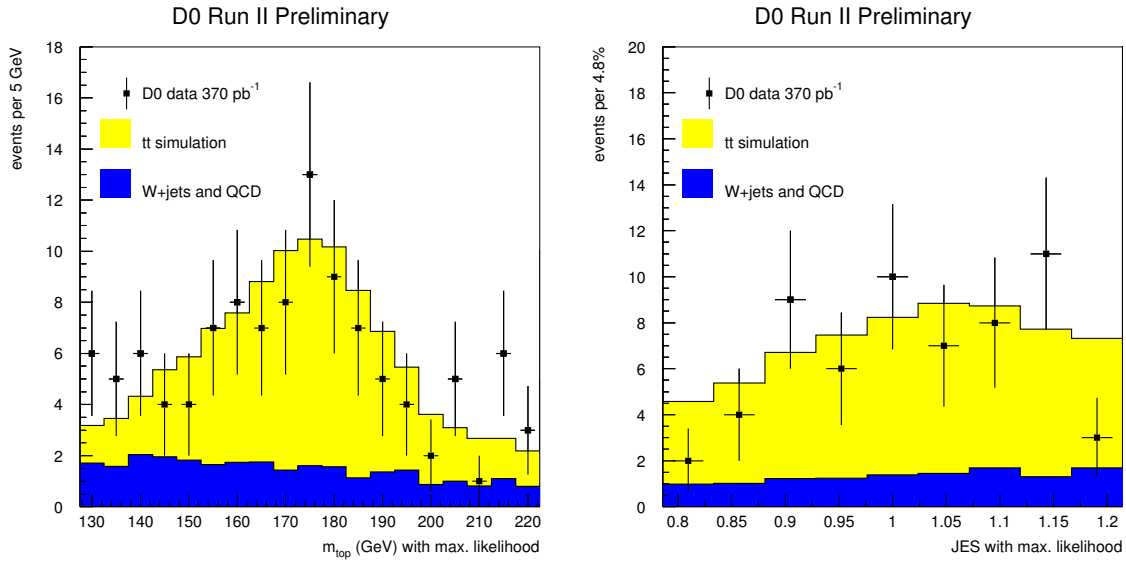

FIG. 13: *The most probable value of the top quark mass (left, for JES=1.0) and JES parameter (right, for $m_{\rm top}$ = 175 GeV) are shown according to the event likelihood, for all events with a combined discriminant $D > 0.3$. Note that these plots only show one number per event and do not convey the full information that is taken into account in the actual likelihood fit.*

Source of uncertainty	Size of the effect (GeV)
Jet Energy Scale (p_T dependence)	+0.45 -0.45
Jet ID efficiency and resolution	0.22
b fragmentation	1.30
b response (h/e)	1.15
b-tagging	0.29
trigger uncertainty	+0.61-0.28
signal modeling	0.73
background modeling	0.20
multi-jet background	0.28
MC calibration	0.25
signal fraction (stat+sys)	0.12
PDF uncertainty	0.023
Total systematic uncertainty	+2.10-2.04
Statistical uncertainty including jet energy scale	4.43
Total uncertainty	+4.90 -4.87

TABLE IV: *Summary of the uncertainties on the Ideogram top quark mass measurement.*

default jet p_T. The value of 0.02 is suggested by the jet+photon studies. The mass obtained with the modified ensembles was compared to the default sample and the shift quoted as a symmetric systematic uncertainty of 0.45 GeV.

- **Jet reconstruction efficiency and resolution:** In addition to uncertainties on the reconstructed jet energies, differences between data and the Monte Carlo simulation in the reconstruction efficiency and jet energy resolution may lead to a mass bias. Both efficiency and resolution were varied as a function of jet p_T and rapidity within estimated uncertainties. No significant effect was observed, with an estimated statistical precision of about 0.15 GeV. For both effects combined an uncertainty of 0.22 GeV is quoted.

- ***b* fragmentation:** While the effect of the overall jet energy scale uncertainty is reduced through the fitting of the JES parameter, differences in the b/light jet energy scale ratio between data and simulation may still affect the measurement. One possible source for such differences could be the description of ***b*** jet fragmentation

in the simulation. Fragmentation effects were studied using simulated $t\bar{t}$ events with different fragmentation models for b jets. The default Bowler [23] scheme with r_t=1.0 is replaced with r_t=0.69 or with Peterson [24] fragmentation with ε_b=0.00191. Ensemble tests are repeated using events from each of the three simulations. The absolute values of the deviations in top quark mass results with respect to the standard sample are added in quadrature and quoted as a symmetric uncertainty of 1.3 GeV.

- ***b/c* semileptonic decays:** The reconstructed energy of b jets containing a semileptonic bottom or charm decay is in general lower than that of jets containing only hadronic decays. This can only be taken into account for jets in which a soft muon is reconstructed. Thus, the fitted top quark mass still depends on the semileptonic b and c decay branching ratios. They have been varied within the bounds given in [25], and the resulting shifts were found to be negligible (evaluated using the Matrix Element method [18]).

- ***b* jet response:** Variations of the h/e calorimeter response lead to additional differences in the b/light jet energy scale ratio between data and simulation. The corresponding uncertainty is estimated to be 1.15 GeV.

- ***b* tagging:** The b tagging rates for b-jets, c-jets and light quark jets are varied within the uncertainties known from the data, and the resulting variations are propagated to the mass. The combined effect is 0.29 GeV.

- **Trigger:** The trigger efficiencies used in the Monte Carlo simulation were varied by their uncertainties estimated from data and the resulting variations in fitted mass summed in quadrature. The combined uncertainty on the calibration amounts to $+0.61$ -0.28 GeV, which is propagated to the measured top quark mass as a systematic uncertainty.

- **Signal modeling:** The main uncertainty in the modeling of $t\bar{t}$ events is related to the radiation of gluons in the production or decay of the $t\bar{t}$ system. A difference in the description of hard gluon radiation could affect the transverse momentum spectrum of the $t\bar{t}$ system, or for example change the rate of confusion between jets from the hadronically decaying W boson and initial state gluons, which could affect the reconstructed top quark mass. To assess the uncertainty related to the modeling of high energy gluons, the difference was studied between the default signal simulation and a dedicated $t\bar{t}$+jet simulation in which an energetic parton is produced in addition to the $t\bar{t}$ system in the production process simulated using ALPGEN. The difference in cross-section calculations between leading and next-to-leading order suggests that such hard gluon radiation may be present in about 35% of $t\bar{t}$ events that pass the event selection. Ensembles were made with the usual composition, but replacing the default $t\bar{t}$ events with the events from the dedicated $t\bar{t}$+jet simulation. 35% of the observed shift in the calibration corresponds to 0.73 GeV, which is assigned as a symmetric systematic uncertainty.

- **Background modeling:** In order to study the sensitivity of the measurement to the choice of background model, the standard W+jets Monte Carlo sample is replaced by an alternative sample with the default factorization scale of $Q^2 = m_W^2 + \sum_j p_{T,j}^2$ replaced by $Q'^2 = \langle p_{T,j} \rangle^2$. Two large ensembles were constructed using the two different background simulations, and the observed difference of 0.20 GeV in fitted mass is assigned as a systematic uncertainty.

- **Multi-jet background:** The W+jets simulation is used to model the small multi-jet background in the selected event sample in the analysis. The systematic uncertainty from this assumption is computed by selecting a dedicated multi-jet enriched sample of events from data by inverting the lepton isolation cut in the event selection. The calibration of the method is repeated with ensembles formed where these events are used to model the multi-jet background, according to the fractions given in table I. The observed shift is 0.33 GeV, which is quoted as a systematic uncertainty.

- **MC calibration:** The statistical uncertainty on the calibration curve shown in Figure 7 is propagated through the analysis and yields a systematic uncertainty on the result of 0.25 GeV.

- **Signal fraction:** The signal fraction in the data sample is varied within the uncertainty determined from the discriminant fit, and the resulting variation of the top quark mass is taken as systematic uncertainty. To determine the uncertainty on the signal fraction, an estimated relative systematic uncertainty of 11% was added in quadrature to the relative statistical uncertainty of 7% of the fit. This excercise, just changing the fraction of $t\bar{t}$ signal in the ensembles, may still underestimate the systematic uncertainty due to the estimated signal fraction, since it still uses a triple discriminant fit with MC templates that are fully consistent with the events used in the ensembles. An additional systematic is assigned to describe a possible systematic bias due to a systematic error in the shape of the templates used. A relative systematic shift of 7% in the fitted purity (with respect to the value preferred by the likelihood fit) was applied in the mass fit, and the shift in fitted mass quoted as a systematic uncertainty. The combined uncertainty, adding the above contributions in quadrature, is 0.12 GeV.

- **PDF uncertainty:** The Ideogram analysis measures the top quark mass directly from the invariant mass of the $t\bar{t}$ decay products without making specific assumptions related to the production process. Nevertheless the calibration of the analysis relies on Monte Carlo simulation in which a certain PDF was used (CTEQ5L). It is conceivable that a different choice of PDF would lead to a slightly different calibration. To study the systematic uncertainty on $m_{\rm top}$ due to the precise PDF description, several PDF uncertainties were considered. PDF variations provided with the next-to-leading-order PDF set CTEQ6M [22] were compared to the default CTEQ6M (no variations for a leading order PDF are available). Furthermore the effect of a variation of α_s was evaluated and the difference between the results obtained with the CTEQ5L and MRST leading order PDFs was taken as another systematic uncertainty. In all cases a large ensemble composed of events generated with CTEQ5L was reweighted such that the distribution corresponding to the desired PDF set was obtained. The difference between weighted and unweighted ensemble was then quoted as systematic uncertainty, and all individual uncertainties are added in quadrature. The resulting combined uncertainty turn out to be very small: $+0.0231$ -0.0234 GeV.

IX. CROSS-CHECK USING EXTERNAL JES CONSTRAINT

As a cross-check the analysis was repeated using the two alternative calibration strategies discussed in section VI E. Fixing the JES parameter in the fit and relying fully on the external JES constraints from jet+photon calibration the top quark mass is measured to be:

$$m_{\rm t} = 175.8 \pm 2.9\ ({\rm stat})^{+2.9}_{-3.4}\ ({\rm syst})\ {\rm GeV}$$

In the second approach the JES parameter is allowed to float freely in the fit but no calibration of the JES slope is applied. Again the external JES constraints from jet+photon calibration are required to set the Jet Energy Scale and remaining JES systematics. Effectively this approach combines in-situ with external JES information, leading to the following result:

$$m_{\rm t} = 173.9 \pm 3.6\ ({\rm stat})^{+2.2}_{-2.0}\ ({\rm syst})\ {\rm GeV}$$

In both cases the systematic uncertainties include the increased JES systematic and the other systematic uncertainties, determined in the same way as described for the main result in section VIII. Comparing the latter (most precise) cross-check with the main result, one can conclude that omitting the external JES constraint and relying fully on the in-situ information changes the central result only by 0.2 GeV. The 2 GeV difference between the first cross-check and the main result correlates very well with the 2.7% difference in JES value obtained with the external and in-situ JES calibrations. This difference is fully covered by the quoted uncertainties.

X. RESULT AND CONCLUSIONS

A measurement of the top quark mass using lepton+jets $t\bar{t}$ events in 370 pb^{-1} of data collected with the D0 detector at Tevatron Run II is presented. The events are analyzed with the Ideogram method, which is designed to extract the maximum kinematic information from the event sample selected. To reduce the dependence on the calibration of the overall jet energy scale, previously the dominant systematic uncertainty, the overall scale factor JES for the energy of reconstructed jets is a free parameter in the fit determined simultaneously with the top quark mass. The measured value of the top quark mass is

$$m_{\rm t} = 173.7 \pm 4.4\ ({\rm stat}\ +\ {\rm JES})^{+2.1}_{-2.0}\ ({\rm syst})\ {\rm GeV}$$

with a fitted JES scaling factor:

$${\rm JES\ factor}\ = 0.989 \pm 0.029\ ({\rm stat\ only})$$

in good agreement with the reference scale (=1.0), with the results from the jet+photon calibration ($\approx$0.962 +0.021 -0.023) and the JES factor fitted by the Matrix Element analysis on the same data set [18]. This result is in good agreement with other top quark mass measurements [2, 11, 12, 18].

Acknowledgments

We thank the staffs at Fermilab and collaborating institutions, and acknowledge support from the DOE and NSF (USA); CEA and CNRS/IN2P3 (France); FASI, Rosatom and RFBR (Russia); CAPES, CNPq, FAPERJ, FAPESP and FUNDUNESP (Brazil); DAE and DST (India); Colciencias (Colombia); CONACyT (Mexico); KRF and KOSEF (Korea); CONICET and UBACyT (Argentina); FOM (The Netherlands); PPARC (United Kingdom); MSMT (Czech Republic); CRC Program, CFI, NSERC and WestGrid Project (Canada); BMBF and DFG (Germany); SFI (Ireland); Research Corporation, Alexander von Humboldt Foundation, and the Marie Curie Program.

[1] D0 CONF note 4574 (2004), http://www-d0.fnal.gov/Run2Physics/WWW/results/prelim/TOP/T08/T08.pdf
[2] V.M. Abazov *et al*, Nature **429**, 638 (2004).
[3] DELPHI Collaboration, Eur. Phys. J. C **2**(1998) 581; DELPHI Collaboration, Phys. Lett. B **462** (1999) 410; DELPHI DELPHI Collaboration, Phys. Lett. B **511** (2001) 159; M. Mulders (DELPHI Collaboration), Int. J. Mod. Phys. A 16S1A (2001) 284; M. Mulders, Ph.D. thesis (FOM, Amsterdam & Amsterdam U.), Sep 2001, 226pp.
[4] V. M. Abazov *et al*, Phys. Lett. B **626**, 45 (2005).
[5] D0 CONF note 4874 (2005), http://www-d0.fnal.gov/Run2Physics/WWW/results/prelim/TOP/T17/T17.pdf
[6] D0 CONF note 5053 (2006), http://www-d0.fnal.gov/Run2Physics/WWW/results/prelim/TOP/T28/T28.pdf
[7] B. Abbott *et al*, Phys. Rev. D **58**, 052001 (1998); S. Abachi, Phys.Lett. B **79**, 1197 (1997).
[8] D0 CONF note 4728 (2005), http://www-d0.fnal.gov/Run2Physics/WWW/results/prelim/TOP/T12/T12.pdf
[9] D0 Collaboration, Phys. Rev. D **72** (2005) 011104.
[10] D0 Collaboration, Phys.Lett. B **626** (2005) 35-44.
[11] F. Abe *et al*, Phys. Rev. Lett. **80**, 2767 (1998); F. Abe *et al*, Phys. Rev. Lett. **80**, 2779 (1998); F. Abe *et al*, Phys. Rev. Lett. **82**, 271 (1999); F. Affolder *et al*, Phys. Rev. D **63**, 032003 (2001); S. Abachi *et al*, Phys. Rev. Lett. **79**, 1197 (1997); B. Abbott *et al*, Phys. Rev. Lett. **80**, 2063 (1998); B. Abbott *et al*, Phys. Rev. D **58**, 052001 (1998); B. Abbott *et al*, Phys. Rev. D **60**, 052001 (1999); V.M. Abazov *et al*, Nature **429**, 638 (2004); V. M. Abazov *et al*, Phys. Lett. B **606**, 25 (2005).
[12] A. Abulencia, *Precision Top Quark Mass Measurement in the Lepton + Jets Topology in ppbar Collisions at sqrt(s) = 1.96 TeV*, hep-ex/0510049, submitted to Phys. Rev. Lett.; A. Abulencia, *Top Quark Mass Measurement Using the Template Method in the Lepton + Jets Channel at CDF II*, hepex/ 0510048, submitted to Phys. Rev. D.
[13] V. Abazov *et al*, *The Upgraded D0 Detector*, physics/0507191, accepted by Nucl. Instrum. Methods Phys. Res. A.
[14] S. Abachi *et al*, Nucl. Instrum. Methods Phys. Res. A **338**, 185 (1994).
[15] V.M. Abazov *et al*, physics/0503151 (2005).
[16] M.L. Mangano *et al*, JHEP 307, 1 (2003).
[17] T. Sjöstrand, P. Eden, C. Friberg, L. Lönnblad, G. Miu, S. Mrenna and E. Norrbin, Computer Phys. Commun. 135, 238 (2001).
[18] P. Schieferdecker, FERMILAB-THESIS 2005-46, publication in preparation.
[19] *SLUO Lectures on Statistics and Numerical Methods in HEP, Lecture 6: Resampling and the Bootstrap*, Roger Barlow *and references therein*, see http://www.hep.man.ac.uk/u/roger/home.html and http://www.hep.man.ac.uk/preprints/manhep99-4.ps
[20] B. Efron, *Computer and the Theory of Statistics*, SIAM Rev.**21**(1979), 460; P. Diaconis and B. Efron, *Computer-Intensive Methods in Statistics*, Scientific American **248:5**(1983), 96; B. Efron and R. J. Tibshirani, *An Introduction to the Bootstrap*, Chapman & Hall, 1993.
[21] H. L. Lai *et al* [CTEQ Collaboration], *Global QCD analysis of parton structure of the nucleon: CTEQ5 parton distributions*, Eur. Phys. J. C 12, 375 (2000).
[22] J. Pumplin *et al*, JHEP 0207, 012 (2002).
[23] M.G. Bowler, Z. Phys C**11**, 169 (1981).
[24] C. Peterson *et al*, Phys. Rev. D**27**, 105 (1983).
[25] The ALEPH, DELPHI, L3, OPAL, and SLD Collaborations, the LEP Electroweak Working Group, SLD Electroweak Group, and SLD Heavy Flavour Group, SLAC-R-774, (2005), hep-ex/0509008.